

One-Dimensional Magnets

DOI: 10.1002/ange.200500464

Molecular Engineering for Single-Chain-Magnet Behavior in a One-Dimensional Dysprosium–Nitronyl Nitroxide Compound***Lapo Bogani, Claudio Sangregorio, Roberta Sessoli, and Dante Gatteschi**

The discovery of single molecule magnets (SMMs), about a decade ago,^[1] opened up a very lively scientific area where still both physicists and chemists join their efforts to better understand and selectively change the magnetic properties of matter.^[2] On one side, the interest aroused by these materials is due to the fact that they allow us to directly address questions of fundamental interest,^[3] and, on the other side, their proposed applications make them appealing candidates for future devices.^[4] The field was further expanded by the discovery, some years ago, of a polymeric compound, [Co(hfac)₂][NIT(C₆H₄OMe)]^[5] (hfac = hexafluoroacetylacetonate; NIT(R): 2-(4'-R)-4,4,5,5-tetramethylimidazoline-1-oxyl-3-oxide), which displays a hysteresis behavior above the temperature of liquid He without undergoing three-

[*] L. Bogani, Dr. C. Sangregorio, Prof. R. Sessoli, Prof. D. Gatteschi
Department of Chemistry and INSTM Research Unit
Università di Firenze
Via della Lastruccia 3, 50019 Sesto Fiorentino (Italy)
Fax: (+39) 055-457-3372
E-mail: dante.gatteschi@unifi.it

[**] This work was financially supported by the Human Potential Program RTN-QUEMOLNA (FP6-504880), the Italian MIUR (FIRB and PRIN projects), and the German DFG (SPP1137). We acknowledge Prof. A. Rettori, Dr. M. G. Pini, and Prof. C. Benelli for many stimulating discussions and Dr. P. Rosa for his assistance in ac magnetic measurements.

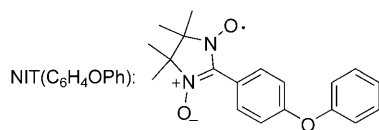


Supporting information for this article is available on the WWW under <http://www.angewandte.org> or from the author.

dimensional (3D) magnetic ordering. This slow dynamics of the magnetization was explained with Glauber's model^[5] for Ising spin chains and, while the physics underlying these systems is revealing interesting aspects,^[6] much effort is devoted to the synthesis of new chain compounds of this kind, known as single-chain magnets (SCMs).^[7] The two requirements needed to observe Glauber dynamics, that is, a strong Ising anisotropy and a very low ratio of interchain/intrachain interactions, are difficult to balance, and only a few compounds have been proposed as SCMs up to now.^[8]

Rare-earth-radical-based chains are very appealing candidates for SCMs owing to the Ising anisotropy of their metallic centers, and $[\text{Dy}(\text{hfac})_3\{\text{NIT}(\text{Et})\}]$ (**1**) displays a transition to 3D magnetic order at 4.3 K.^[9] However, the interchain interactions are relatively weak, as the shortest metal–metal distances are 10.76 Å, and only through-space (dipolar) interchain interactions are active. It should be possible to further increase these distances by varying the radical, thus determining a passage from 3D order to SCM behavior. This can shed light on the delicate balance between the exchange, structural features, and magnetic anisotropy required for SCM behavior. This idea proved to work well, and we wish to report herein the first complete structural and magnetic characterization of a rare-earth-based SCM synthesized by a rational approach. Frequency-dependent data on a Tb-based compound have been reported in a previous work, but structural evidence was lacking.^[10]

The radical $\text{NIT}(\text{C}_6\text{H}_4\text{OPh})$ was an appealing candidate to increase the separation of neighboring chains because it possesses two rather mobile aromatic rings, as spacers, and an



ether group in between that enriches the electron density of these rings. The presence of such electron-rich groups alternating with the electron-poor rings formed when hfac ligands coordinate to a metal center favors stacking interactions along the chain, thus stabilizing the polymeric compound.^[11]

The reaction of $[\text{Dy}(\text{hfac})_3(\text{H}_2\text{O})_2]$ with the $\text{NIT}(\text{C}_6\text{H}_4\text{OPh})$ radical in hot *n*-heptane afforded single crystals of the chain compound $[\text{Dy}(\text{hfac})_3\{\text{NIT}(\text{C}_6\text{H}_4\text{OPh})\}]$ (**2**) suitable for X-ray analysis. This compound, whose structure is depicted in Figure 1,^[12] consists of chains, parallel to *b*, of octacoordinated $\text{Dy}(\text{hfac})_3$ centers connected by radical units, which act as bis-monodentate ligands.

The coordination geometry around the Dy atom is a distorted dodecahedron with triangular faces, where the two radical oxygen atoms occupy the apical positions of two distorted pentagons. The distances between the metal center and these oxygen atoms were found to be very similar to each other (2.329(4) Å and 2.385(4) Å). The stacking interactions between the inner aromatic ring of the spacer and an hfac ligand can be clearly identified,^[13] as the distance between the two aromatic planes is 3.75(5) Å and the angle between them

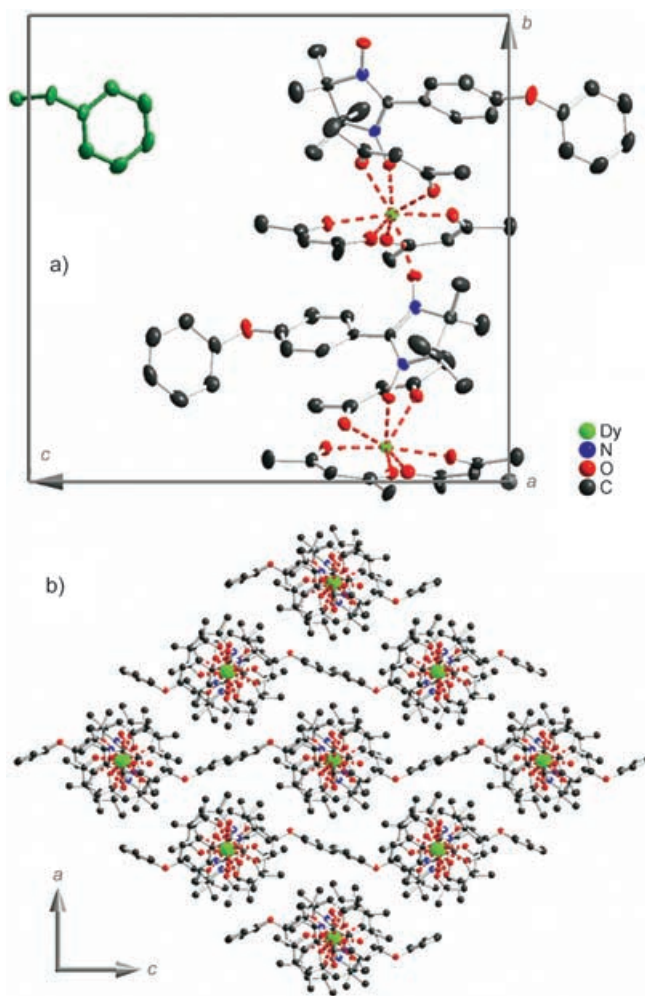


Figure 1. Views of the structure of **2**: a) along the *a* axis, showing the chain structure together with the unit cell. The aromatic tail of the radical of an adjacent chain is also shown (in green); b) along the crystallographic *b* axis, showing the packing of the chains. Ellipsoids are drawn at 50% probability and fluorine and hydrogen atoms have been omitted for clarity.

is 14.6(2)°, in agreement with the situation observed in other metal $\text{NIT}(\text{R})$ derivatives.^[11] The outer aromatic ring of the spacer, on the other hand, is placed between the chains, with the normal tilted with respect to the inner ring (65.84°) and oriented almost perpendicularly to the chain axis (86.71°). This ring lies isolated in a niche between two other chains, surrounded by the fluorine atoms of four hfac ligands, with a distance of 5.90(5) Å from the centroid of the nearest ligand. In this way, as can be observed from Figure 1, the free volume between the chains is alternatively occupied by the spacers of two different chains, thereby minimizing any weak magnetic interactions between the radicals. Our strategy leads to an increased volume per metal center, which grows from 881 Å³ in **1** to 1001 Å³ in **2** and, more importantly, to a lengthening of all distances between different chains. Analysis of the distances between a chain and the six neighboring ones showed the presence, in both cases, of three couples of equally distant chains. All three distances increase, with the shortest distance between two Dy centers growing from 10.76

11.35 Å, and the next two shortest separations increasing from 11.23 to 11.38 Å and from 11.43 to 14.31 Å. In other words, there is a change from a pseudo-hexagonal arrangement of the chains in **1** to a pseudo-tetragonal one in **2**. Considering the r^{-3} dependence of magnetic dipolar interactions, such changes in the crystal structure, although they may not seem dramatic, reduce the interactions along the shortest distance by 15 % and those along the longest distance by up to 49 %. This analysis reveals that the engineering of the compound has led to an efficient suppression of interchain interactions independent of the orientation of the magnetic easy axis.

The effect of this crystal engineering strategy on the magnetic properties is evident from Figure 2, in which we show the dc magnetic susceptibility measured for a powder

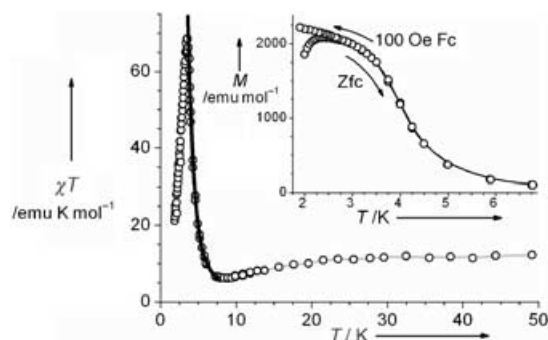


Figure 2. Low-temperature dependence of the χT product from dc magnetic measurements performed in a 100 Oe applied field. The black line represents the calculated curve, as described in the text. In the inset we show the gap that opens up below 2.6 K between the zero-field-cooled and the 100-Oe-cooled curves.

sample. The radicals are $S = 1/2$ isotropic magnetic centers, while Dy^{III} , a $^6\text{H}_{15/2}$ ion, is usually treated, at low temperature, as an effective $S = 1/2$ anisotropic center. The high-temperature χT value, 12.2 emu K mol^{-1} at 300 K, is slightly lower than the expected theoretical value for two such noninteracting magnetic centers, but consistent with the data available for **1**.^[9] The temperature dependence of χT shows a minimum at 8.6 K and a rounded peak of 68.5 emu K mol^{-1} at 3.6 K, typical of 1D behavior, while the cusp found in the 3D-ordered compound^[9] is not observed.

The magnetism of this type of lanthanide–radical chain is characterized by the presence of nearest-neighbor (NN) ferromagnetic metal–radical and next-nearest-neighbor (NNN) antiferromagnetic metal–metal or radical–radical magnetic couplings (J_{Mr} , J_{MM} , and J_{rr} , respectively).^[9] The overall behavior at low temperature depends on the ratio between ferro- and antiferromagnetic interactions.^[14] The low-temperature powder data of **2** suggest that ferromagnetic interactions dominate. A scaling procedure of the χT data^[15] clearly indicates a linear regime characteristic of Ising 1D systems (see Supporting Information). The data between 8.5 and 3.6 K were therefore reproduced with a spin-1/2 Ising model with alternating Landé g -factors (g_{r} and g_{Dy} for the radical and the Dy centers, respectively) and three exchange interactions. A good agreement ($R = 0.999$) between the

calculated and experimental curves in this region was found with the values $g_{\text{r}} = 2.0$, $g_{\text{Dy}} = 8.0$ (vide infra), ferromagnetic $J_{\text{Mr}} = 19$ K, and antiferromagnetic $J_{\text{rr}} = -6.5$ and $J_{\text{MM}} = -4$ K. A similar agreement was also observed with other sets of parameters, thereby suggesting a strong correlation between them, with the difference between the ferromagnetic and antiferromagnetic interactions being the key point. Moreover, due to the presence of a strong anisotropy of the magnetization, single-crystal measurements as a function of the orientation will be needed to give a completely reliable set of values.

1D Ising systems are expected to follow Glauber slow dynamics with a thermally activated reversal of the magnetization, $\tau = \tau_0 \exp(\Delta/k_{\text{B}}T)$, where the energy barrier, Δ , depends on the exchange interaction, that is, $\Delta = |J|$ for $S = 1/2$. The ac magnetic susceptibility curves, measured in zero static field, display a frequency-dependent peak for both in-phase χ' and out-of-phase χ'' signals below 4.5 K, as shown in Figure 3, thus indicating the presence of a thermally activated mechanism. A frequency-independent peak at the transition

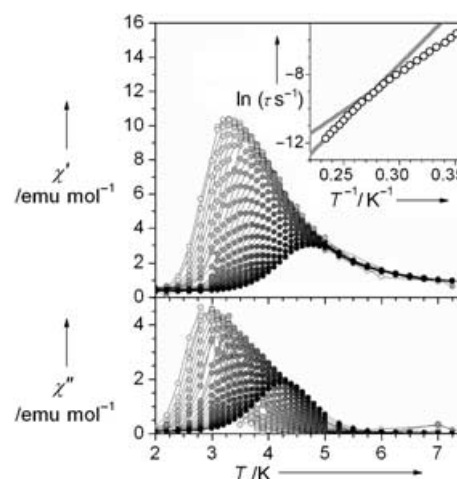


Figure 3. Temperature dependence of the real (top) and imaginary (bottom) components of the ac magnetic susceptibility measured in zero applied field in the frequency range 25 Hz–20 kHz. The inset shows the obtained Arrhenius plot and the crossover.

temperature would be found for a 3D-ordered compound. The dynamic behavior of **2** can be reproduced with the generalized Debye model (Supporting Information) by taking into account a narrow distribution of relaxation times, $\alpha = 0.16$, a value compatible with those observed for other SCMs.^[8]

The Arrhenius plot extracted from these data, reproduced in the inset of Figure 3, shows the presence of a crossover between two different activated regimes, both of which give best-fits with physical τ_0 values (5.6×10^{-10} and 1.9×10^{-12} s for the low- and high-temperature regimes, respectively) and two different barriers (42 and 69 K, respectively). The presence of a crossover in the Arrhenius plot of SCMs that halves the Glauber activation barrier due to finite-size effects has been predicted^[16] and experimentally observed for systems with a slow relaxation of single monomeric units.^[15]

Below 2.6 K, irreversibility effects also appear in static magnetic measurements as a discrepancy between the magnetization curve cooled in zero field and the curve cooled in an applied external field, as shown in the inset of Figure 2. The magnetization curve taken at 1.60 K, depicted in Figure 4, reveals the opening of a hysteresis loop and a very rich magnetic behavior with two different steps, an unprece-

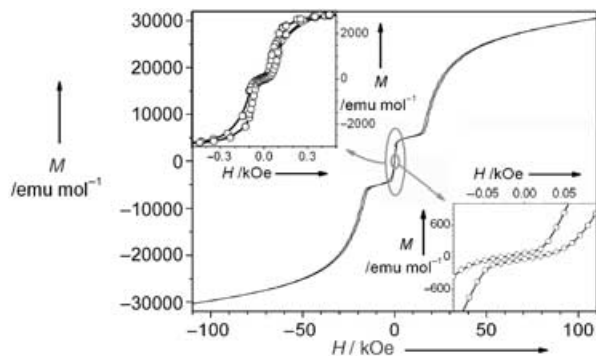


Figure 4. Magnetization curve versus applied field measured at 1.60 K. The nested hysteresis cycles are shown in the two insets.

dent feature in rare-earth polymeric systems. The fact that such steps do not change on varying the field sweep rate indicates that they are associated with static properties. While we cannot totally exclude that the first step around $H = 50$ Oe is due to residual antiferromagnetic interchain interactions, it is interesting to note that the slow relaxation of the magnetization observed above 2 K in zero field also persists above the step. This is consistent with a very “robust” Glauber dynamic regime that is unaffected by possible weak interchain interactions.^[17]

The step at around $H = 15$ kOe is more difficult to rationalize. The presence of competing NN and NNN interactions could stabilize states that do not correspond to the ferromagnetic alignment of all the spins. A state that has been previously discussed can be described by the spin arrangement $\dots\downarrow\uparrow\downarrow\uparrow\downarrow\uparrow\dots$, in which the red arrows represent Dy magnetic moments and the black arrows represent radical sites.^[9] This state has a magnetization corresponding to $(M_{\text{Dy}} - M_r)/3$, and is not too far from that observed in Figure 4, assuming that the high-field value tends to $(M_{\text{Dy}} + M_r)$, thus providing an average g_{Dy} value of around 8. However, we could not successfully reconcile this picture with the ferromagnetic behavior observed between 4 and 10 K using a simple Ising model; further investigations with single crystals are necessary to clarify this point.

In conclusion, we have prepared and structurally characterized the first rare-earth-radical-based coordination polymer to exhibit SCM behavior, namely $[\text{Dy}(\text{hfac})_3\{\text{NIT}(\text{C}_6\text{H}_4\text{OPh})\}]$ (**2**). A critical reconsideration of previously known compounds was a key point to rationally plan the synthesis to enhance the stacking along the chains and to weaken the interchain magnetic interactions. To the best of our knowledge, this is the first successful preparation of an SCM from a material known to undergo 3D magnetic ordering. The chains exhibit all the features of a slowly

relaxing system, including a crossover between two Arrhenius regimes, and a hysteresis loop opens below 3 K. The observation of such a crossover in **2**, if due to finite-size effects, would suggest a significant contribution to the barrier coming from the anisotropic building blocks, as the barrier is not exactly halved.^[15] This would open the possibility to study the effect of the recently observed dynamics of rare-earth single-ion units^[18] when arranged in chains. These dynamic features are accompanied by a very rich static behavior that could be due to the interplay of NN and NNN interactions, with the presence of several low-energy states. Finally, thanks to the synthetic possibilities opened up here, the chemical reactivity of rare-earth metals can now be exploited to study the role of the anisotropy and magnetic multiplicity of the rare-earth ion on the slow dynamics of both monomers and chains.

Experimental Section

Synthesis of 2: $[\text{Dy}(\text{hfac})_3(\text{H}_2\text{O})_2]$ (1 mmol) was dissolved in boiling dry *n*-heptane (30 mL). The solution was left to boil for 20 min and then cooled down to 75 °C, whereupon 1 mmol of the crystalline solid radical $\text{NIT}(\text{C}_6\text{H}_4\text{OPh})$ was slowly added whilst stirring followed by 3 mL of CH_2Cl_2 . The final solution was cooled down to room temperature and was left to stand for about 24 h to give green, needle-like crystals. $\text{C}_{34}\text{H}_{24}\text{DyF}_{18}\text{N}_2\text{O}_9$: calcd C 36.89, H 2.18, N 2.52; found: C 37.10, H 2.50, N 2.79.

Physical measurements: The dc magnetic susceptibility measurements were performed on solid polycrystalline samples with a Cryogenic S600 SQUID magnetometer and were all corrected for the diamagnetic contribution as calculated with Pascal's constants. Magnetization curves with fields over 60 kOe were measured with an Oxford VSM system after inclusion of the sample in grease to prevent orientation of the crystallites. Data were corrected for the magnetism of the grease, which was independently determined at the same temperature and fields. The ac magnetic susceptibility was measured by using a homemade probe operating in the range 20–20 000 Hz.^[19] Crystal structure data were collected with an Oxford Diffraction Xcalibur3 diffractometer.

Received: February 7, 2005

Revised: June 6, 2005

Published online: August 5, 2005

Keywords: lanthanides · magnetic properties · one-dimensional magnets · radicals · rational synthesis design

- [1] R. Sessoli, D. Gatteschi, A. Caneschi, M. A. Novak, *Nature* **1993**, 365, 141.
- [2] D. Gatteschi, R. Sessoli, *Angew. Chem.* **2003**, 115, 278; *Angew. Chem. Int. Ed.* **2003**, 42, 268.
- [3] a) P. C. E. Stamp, *Nature* **1996**, 383, 125; b) E. M. Chudnovsky, *Science* **1998**, 280, 229; c) W. Wernsdorfer, R. Sessoli, *Science* **1999**, 284, 133.
- [4] M. N. Leuenberger, D. Loss, *Nature* **2001**, 410, 789.
- [5] A. Caneschi, D. Gatteschi, N. Lalioti, C. Sangregorio, R. Sessoli, G. Venturi, A. Vindigni, A. Rettori, M. G. Pini, M. A. Novak, *Angew. Chem.* **2001**, 113, 1810; *Angew. Chem. Int. Ed.* **2001**, 40, 1760.
- [6] L. Bogani, A. Caneschi, M. Fedi, D. Gatteschi, M. Massi, M. A. Novak, M. G. Pini, A. Rettori, R. Sessoli, A. Vindigni, *Phys. Rev. Lett.* **2004**, 92, 207204.

- [7] R. Clerac, H. Miyasaka, M. Yamashita, C. Coulon, *J. Am. Chem. Soc.* **2002**, *124*, 12837.
- [8] a) R. Lescouezec, J. Vaissermann, C. Ruiz-Perez, F. Lloret, R. Carrasco, M. Julve, M. Verdaguer, Y. Dromzee, D. Gatteschi, W. Wernsdorfer, *Angew. Chem.* **2003**, *115*, 1521; *Angew. Chem. Int. Ed.* **2003**, *42*, 1483; b) T. Liu, D. Fu, S. Gao, Y. Zhang, H. Sun, G. Su, Y. Liu, *J. Am. Chem. Soc.* **2003**, *125*, 13976; c) L. M. Toma, R. Lescouezec, F. Lloret, M. Julve, J. Vaissermann, M. Verdaguer, *Chem. Commun.* **2003**, 1850; d) E. Pardo, R. Ruiz-Garcia, F. Lloret, J. Faus, M. Julve, Y. Journaux, F. Delgado, C. Ruiz-Perez, *Adv. Mater.* **2004**, *16*, 1597.
- [9] a) C. Benelli, A. Caneschi, D. Gatteschi, R. Sessoli, *Adv. Mater.* **1992**, *4*, 504; b) C. Benelli, A. Caneschi, D. Gatteschi, R. Sessoli, *Inorg. Chem.* **1993**, *32*, 4797; c) C. Benelli, A. Caneschi, D. Gatteschi, R. Sessoli, *J. Appl. Phys.* **1993**, *73*, 5333; d) C. Benelli, A. Caneschi, D. Gatteschi, L. Pardi, P. Rey, *Inorg. Chem.* **1990**, *29*, 4223.
- [10] J. P. Costes, J. M. Clemente-Juan, F. Dahan, J. Milon, *Inorg. Chem.* **2004**, *43*, 8200.
- [11] A. Caneschi, D. Gatteschi, N. Lalioti, C. Sangregorio, R. Sessoli, *J. Chem. Soc. Dalton Trans.* **2000**, 3907.
- [12] Crystal structure data for **2**: $C_{34}H_{24}DyF_{18}N_2O_9$ ($0.28 \times 0.09 \times 0.02 \text{ mm}^3$), $M_r = 1109.05$, orthorhombic, space group $P2_12_12_1$ (no. 19), $a = 14.313(1)$, $b = 16.472(1)$, $c = 16.974(1) \text{ \AA}$, $V = 4001.9(6) \text{ \AA}^3$, $Z = 4$, $\rho_{\text{calcd}} = 1.841 \text{ g cm}^{-3}$, $\mu = 2.006 \text{ mm}^{-1}$, $\text{min./max. transmission} = 0.675$, $\text{MoK}\alpha$ radiation ($\lambda = 0.71069 \text{ \AA}$), $T = 150 \text{ K}$, 25285 collected reflections of which 7273 were unique ($R_{\text{int}} = 0.0397$), and 574 parameters, $R1 = 0.0338$ and $wR2 = 0.0694$ using 5565 reflections with $I > 2\sigma(I)$, $R1$ (all data) = 0.0449, $\text{GooF} = 0.947$. Lorentzian polarization and absorption corrections were applied to the data set. The structure was solved by direct methods (SIR97), and was refined by Fourier difference syntheses using SHELXL97 with a full-matrix least-squares method against $|F^2|$ data. During the final iterations, hydrogen atoms were added in calculated positions assuming idealized bond geometries. CCDC-262704 contains the supplementary crystallographic data for this paper. These data can be obtained free of charge from the Cambridge Crystallographic Data Centre via www.ccdc.cam.ac.uk/data_request/cif.
- [13] C. Janiak, *J. Chem. Soc. Dalton Trans.* **2000**, 3885.
- [14] a) M. G. Pini, A. Rettori, *Phys. Rev. B* **1993**, *48*, 3240; b) I. Harada, *J. Phys. Soc. Jpn.* **1983**, *52*, 4099.
- [15] a) C. Coulon, R. Clerac, L. Lecren, W. Wernsdorfer, H. Miyasaka, *Phys. Rev. B* **2004**, *69*, 132408; b) M. Ferbinteanu, H. Miyasaka, W. Wernsdorfer, K. Nakata, K. Sugiura, M. Yamashita, C. Coulon, R. Clerac, *J. Am. Chem. Soc.* **2005**, *127*, 3090.
- [16] a) J. Kamphorst Leal da Silva, A. G. Moreira, M. Silvério - Soares, F. C. Sá Barreto, *Phys. Rev. E* **1995**, *52*, 4527; b) J. H. Luscombe, M. Luban, J. P. Reynolds, *Phys. Rev. E* **1996**, *53*, 5852.
- [17] S. Zümer, *Phys. Rev. B* **1980**, *21*, 1298.
- [18] a) R. Giraud, W. Wernsdorfer, A. M. Tkachuk, D. Mailly, B. Barbara, *Phys. Rev. Lett.* **2001**, *87*, 057203; b) N. Ishikawa, M. Sugita, T. Ishikawa, S. Koshihara, Y. Kaizu, *J. Am. Chem. Soc.* **2003**, *125*, 8694; c) T. Ishikawa, M. Sugita, W. Wernsdorfer, *J. Am. Chem. Soc.* **2005**, *127*, 3650; d) T. Ishikawa, M. Sugita, W. Wernsdorfer, *Angew. Chem.* **2003**, *115*, 2991; *Angew. Chem. Int. Ed.* **2005**, *44*, 2931.
- [19] S. Midollini, A. Orlandini, P. Rosa, L. Sorace, *Inorg. Chem.* **2005**, *44*, 2060.